

# Dalton Transactions

Accepted Manuscript



This article can be cited before page numbers have been issued, to do this please use: M. S. Dimitrijevic, J. Bogdanovic Pristov, M. Zizic, D. M. Stankovi, D. Bajuk-Bogdanovic, M. Stanic, S. Spasic, W. R. Hagen and I. Spasojevic, *Dalton Trans.*, 2019, DOI: 10.1039/C8DT04724C.



This is an Accepted Manuscript, which has been through the Royal Society of Chemistry peer review process and has been accepted for publication.

Accepted Manuscripts are published online shortly after acceptance, before technical editing, formatting and proof reading. Using this free service, authors can make their results available to the community, in citable form, before we publish the edited article. We will replace this Accepted Manuscript with the edited and formatted Advance Article as soon as it is available.

You can find more information about Accepted Manuscripts in the [author guidelines](#).

Please note that technical editing may introduce minor changes to the text and/or graphics, which may alter content. The journal's standard [Terms & Conditions](#) and the ethical guidelines, outlined in our [author and reviewer resource centre](#), still apply. In no event shall the Royal Society of Chemistry be held responsible for any errors or omissions in this Accepted Manuscript or any consequences arising from the use of any information it contains.

## Biliverdin-copper complex at physiological pH

Milena S. Dimitrijević,<sup>a</sup> Jelena Bogdanović Pristov,<sup>a</sup> Milan Žižić,<sup>a</sup> Dalibor M. Stanković,<sup>bc</sup> Danica Bajuk-Bogdanović,<sup>d</sup> Marina Stanić,<sup>a</sup> Snežana Spasić,<sup>e</sup> Wilfred Hagen,<sup>f</sup> Ivan Spasojević<sup>a\*</sup>

Received 00th January 20xx,  
Accepted 00th January 20xx

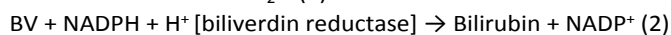
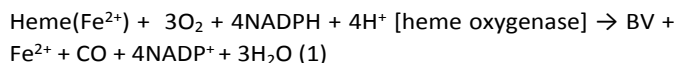
DOI: 10.1039/x0xx00000x

www.rsc.org/

Biliverdin (BV), a product of heme catabolism, is known to interact with transition metals, but the details of such interactions under physiological conditions are scarce. Herein, we examined coordinate/redox interactions of BV with Cu<sup>2+</sup> in phosphate buffer at pH 7.4, using spectrophotometry, HESI-MS, Raman spectroscopy, <sup>1</sup>H NMR, EPR, fluorimetry, and electrochemical methods. BV formed a stable coordination complex with copper in 1:1 stoichiometry. The structure of BV was more planar and energetically stable in the complex. The complex showed strong paramagnetic effects that were attributed to an unpaired delocalized e<sup>-</sup>. The delocalized electron may come from BV or Cu<sup>2+</sup>, so the complex is formally composed either of BV radical cation and Cu<sup>1+</sup> or of BV radical anion and Cu<sup>3+</sup>. The complex underwent oxidation only in the presence of both O<sub>2</sub> and an excess of Cu<sup>2+</sup>, or a strong oxidizing agent, and it was resistant to reducing agents. The biological effects of the stable BV metallocomplex containing a delocalized unpaired electron should be further examined, and may provide an answer to the long-standing question of high energy investment in the catabolism of BV, which represents a relatively harmless molecule *per se*.

### Introduction

Heme, iron protoporphyrin IX complex, is released from hemoglobin in senescent and impaired erythrocytes.<sup>1</sup> It is further subjected to enzymatic degradation to biliverdin (BV) (1), which is rapidly converted to bilirubin by BV reductase (2).



It is still not clear why physiologically harmless BV, which may be easily excreted without conjugation,<sup>2</sup> requires energetically expensive two-electron reduction to potentially toxic bilirubin.<sup>3</sup> A potential explanation may reside in the coordinate and/or redox interactions of BV with copper and other

physiologically-relevant metals.<sup>4</sup> However, the interactions of BV with copper ions have not been examined in physiological settings. Previous studies have performed the synthesis/analysis of BV-copper complexes in organic solvents,<sup>5</sup> in aqueous medium at a very high pH,<sup>6</sup> or using Tris buffer,<sup>7</sup> which shows high affinity for Cu<sup>2+</sup> and may interfere with the interactions with BV.<sup>8</sup> It is important to point out that at physiological pH, BV is present in the dianion form with deprotonated carboxyl groups.<sup>9</sup>

In the present study we applied spectroscopic, (para)magnetic resonance, and electrochemical methods to elucidate the structure and redox properties of complex of BV with copper ions under physiological conditions using phosphate buffer with pH 7.4. Our results imply the formation of a BV radical-copper complex containing a delocalized unpaired electron.

### Results and discussion

UV-Vis spectrophotometry was applied to investigate formation/degradation of complex of BV with copper ions at pH 7.4 (Fig. 1). BV showed bands with  $\lambda_{\text{max}}$  at 315 nm (non-restricted open-chain bilatriens), 375 nm (Soret-like band), and 670 nm (transitions in C=C and C=N systems).<sup>10</sup> Different [BV]/[Cu<sup>2+</sup>] concentration ratios were applied to evaluate the stoichiometry (Fig. 1a). At [BV]/[Cu<sup>2+</sup>] = 2, an immediate decrease in the intensity of the  $\lambda_{670}$  absorption band was observed. At [BV]/[Cu<sup>2+</sup>] = 1, the  $\lambda_{670}$  band was absent, whereas the  $\lambda_{375}$  peak was shifted to 400 nm. It is noteworthy that a new band emerged at ~800 nm. The spectrum for [BV]/[Cu<sup>2+</sup>] = 2 corresponded to the sum of experimental spectra for [BV]/[Cu<sup>2+</sup>] = 1 and BV. The signal in the presence

<sup>a</sup> Department of Life Sciences, Institute for Multidisciplinary Research, University of Belgrade, Kneza Višeslava 1, 11030 Belgrade, Serbia

<sup>b</sup> The Vinča Institute of Nuclear Sciences, University of Belgrade, POB 522, 11001 Belgrade, Serbia

<sup>c</sup> Innovation Center of the Faculty of Chemistry, University of Belgrade, Studentski trg 12-16, 11158 Belgrade, Serbia

<sup>d</sup> Faculty of Physical Chemistry, University of Belgrade, Studentski trg 12-16, 11158 Belgrade, Serbia

<sup>e</sup> Department of Chemistry, Institute of Chemistry, Technology and Metallurgy, University of Belgrade, Studentski trg 12-16, 11158 Belgrade, Serbia

<sup>f</sup> Department of Biotechnology, Delft University of Technology, Van der Maasweg 9, 2629HZ Delft, The Netherlands.

\*Corresponding author: Ivan Spasojević

E-mail: redoxsci@gmail.com.

†Electronic Supplementary Information (ESI) available: [UV-Vis spectra of different BV/copper systems, BV/copper system in DMSO – UV-Vis and <sup>1</sup>H NMR spectra, speciation of Cu<sup>2+</sup> in phosphate buffer, ESI-MS spectrum, scan rate analysis of BV and BV-Cu complex, list of Raman bands for BV.]. See DOI: 10.1039/x0xx00000x

of an excess of  $\text{Cu}^{2+}$  ( $[\text{BV}]/[\text{Cu}^{2+}] = 0.5$ ) was similar to the  $[\text{BV}]/[\text{Cu}^{2+}] = 1$  system. Altogether, this implies that BV interacted with  $\text{Cu}^{2+}$  in 1:1 stoichiometry, which was further confirmed by titration (Fig. 1e). The same stoichiometry of BV (analog)/copper complexes has been observed in organic solvents.<sup>5</sup> The reaction was over within 5 min and all signals were stable under anaerobic conditions for at least one hour. The  $[\text{BV}]/[\text{Cu}^{2+}] = 2$  system was also stable in the presence of  $\text{O}_2$  (Fig. 1b), which implies that the complex is not susceptible to oxidation by  $\text{O}_2$  *per se*. On the other hand, signals for  $[\text{BV}]/[\text{Cu}^{2+}] = 1$  and  $[\text{BV}]/[\text{Cu}^{2+}] = 0.5$  systems showed a decay with time under aerobic settings (Fig. 1c, d). The decrease was more pronounced for the latter. It appears that the complex undergoes oxidation/degradation only in the presence of both  $\text{O}_2$  and 'free'  $\text{Cu}^{2+}$ , which is present in traces in the  $[\text{BV}]/[\text{Cu}^{2+}] = 1$  system, and in excess in the  $[\text{BV}]/[\text{Cu}^{2+}] = 0.5$  system. In the  $[\text{BV}]/[\text{Cu}^{2+}] = 2$  system, BV sequestered (almost) all available copper thus preventing the oxidation.

**Figure 1.** Changes in UV-Vis spectra of biliverdin (BV) in the presence of  $\text{Cu}^{2+}$  in phosphate buffer (50 mM; pH 7.4). (a) Different concentration ratios under anaerobic conditions (Ar atmosphere). Spectra were recorded after 5 min of incubation and remained stable for at least 60 min. (b) The system with  $[\text{BV}]/[\text{Cu}^{2+}] = 2$  molar ratio under aerobic conditions. (c)  $[\text{BV}]/[\text{Cu}^{2+}] = 1$  under aerobic conditions. (d)  $[\text{BV}]/[\text{Cu}^{2+}] = 0.5$  under aerobic conditions. (e) Absorbance titration curve. Spectra were obtained after 5 min incubation period. In all experiments  $[\text{BV}] = 20 \mu\text{M}$ .

The sensitivity of complexes of  $\text{Cu}^{2+}$  and porphyrin model molecules to  $\text{O}_2$  has been observed previously in organic solvents.<sup>5,11</sup> However, the involvement of 'free'  $\text{Cu}^{2+}$  has not been taken into consideration. It is important to point out that the complex was not affected by bathocuproine, a copper chelating agent (ESI Fig. S1<sup>+</sup>), implying that copper cannot be easily removed from the complex. Further, we observed that BV degradation at  $[\text{BV}]/[\text{Cu}^{2+}] = 1$  molar ratio was promoted at higher BV and  $\text{Cu}^{2+}$  concentrations (ESI Fig. S2<sup>+</sup>). This is most likely related to a higher amount of 'free' copper ions and/or to different  $\text{Cu}^{2+}$  speciation in phosphate buffer at different  $[\text{Cu}^{2+}]$  (ESI Fig. S3<sup>+</sup>). The degradation of the complex at high concentrations was prevented by an excess of BV (in the  $[\text{BV}]/[\text{Cu}^{2+}] = 2$  system). Therefore, we applied a  $[\text{BV}]/[\text{Cu}^{2+}] = 2$  molar ratio for methods/measurements that required high concentrations and longer recording periods at room T. It is worth mentioning that the interactions of porphyrins with metals are frequently studied in DMSO, which is a more

**Figure 2.** Structural analysis of biliverdin (BV) interactions with copper ions in phosphate buffer (50 mM; pH 7.4). (a) ESI-MS spectra, full scan positive mode. Proposed structure of the BV-Cu complex is illustrated on the right. The concentrations of BV and copper ions were  $20 \mu\text{M}$ . (b) Raman spectra of BV (1 mM) and  $[\text{BV}]/[\text{Cu}^{2+}] = 2$  system. Raman spectra of  $\text{Cu}^{2+}$  (0.5 mM) and phosphate buffer are presented for reference. Fluorescence-corrected spectra were obtained after 5 min incubation period using the  $\lambda = 532 \text{ nm}$  laser excitation line.

Stronger bands at  $1480 \text{ cm}^{-1}$  (stretching of aliphatic C-C bonds),  $\sim 1580 \text{ cm}^{-1}$  (stretching of C=C bonds in the ring), and  $\sim 1630 \text{ cm}^{-1}$  (stretching of C=C and C=O bonds in the ring), imply higher delocalization of  $\pi$ -electrons and consequently a higher stability of the BV structure. Pertinent to this, it has been proposed that complexes of BV model compounds with  $\text{Cu}^{2+}$  may show unusual electronic structures that exhibit a significant ligand radical character.<sup>16</sup>

Figure 3a shows  $^1\text{H}$  NMR spectrum of BV in phosphate buffer (prepared with  $\text{D}_2\text{O}$ ). Poor resolution of signals, which may

convenient solvent for some analyses. Pertinent to this, BV showed similar UV-Vis spectra in DMSO and phosphate buffer (ESI Fig. S4<sup>+</sup>). However, spectral features of the  $[\text{BV}]/[\text{Cu}^{2+}] = 1$  system differed significantly. The 660 nm band was still present, whereas the 380 nm band showed a decrease and developed a "shoulder" at approximately 440 nm. This implied that the interactions of BV with  $\text{Cu}^{2+}$  in DMSO and in phosphate buffer differ, and pointed out the importance of analysing BV/ $\text{Cu}^{2+}$  system in the aqueous medium.

HESI-MS analysis confirmed that BV built a complex with copper ions in 1:1 stoichiometry (Fig. 2a). The mass spectrum of BV showed a pseudomolecular ion  $[\text{M} + \text{H}]^+$  at  $m/z$  583.07. In the presence of  $\text{Cu}^{2+}$  in 1:1 molar ratio, a peak at  $m/z$  643.36 emerged, whereas the peak of free BV was absent. This  $m/z$  value corresponded to the sum of masses of BV and copper  $[\text{M} + \text{H} + \text{Cu} - 3\text{H}]^+$ . HESI-MS of the  $[\text{BV}]/[\text{Cu}^{2+}] = 0.5$  system showed a significantly higher number of detectable fragments compared to other systems (ESI Fig. S5<sup>+</sup>), further confirming that the complex and BV undergo oxidation/degradation in the presence of  $\text{O}_2$  and an excess of  $\text{Cu}^{2+}$ . Next, we applied Raman spectroscopy (Fig. 2b). The Raman spectrum of BV was in good agreement with previous reports (ESI Table S1<sup>+</sup>). Comparing spectra of BV and BV-Cu complex, the following differences were observed: (i) a new band at  $540 \text{ cm}^{-1}$  emerged for the complex; (ii) the band at  $844 \text{ cm}^{-1}$  was shifted to  $821 \text{ cm}^{-1}$ ; (iii) the peak at  $1303 \text{ cm}^{-1}$  was (almost) absent; (iv) the band at  $1333 \text{ cm}^{-1}$  was stronger; (v) the line at  $1480 \text{ cm}^{-1}$  was stronger; (vi) it appears that two peaks/shoulders of  $1616 \text{ cm}^{-1}$  band emerged/were stronger at  $\sim 1580 \text{ cm}^{-1}$  and  $\sim 1630 \text{ cm}^{-1}$ . The  $540 \text{ cm}^{-1}$  band may be attributed to Cu-N bond vibration.<sup>12</sup> The band at  $844 \text{ cm}^{-1}$  was attributed to ring (C-C bond) stretching.<sup>13</sup> The shift to lower energies implicates increased stability of BV in the complex. The band at  $1303 \text{ cm}^{-1}$  may be attributed to wagging vibration of C-H bond,<sup>13</sup> which are very sensitive to environmental factors.<sup>14</sup> The  $1333 \text{ cm}^{-1}$  band has been previously identified as a structure-sensitive band for Cu-bilirubin complex, and has been attributed to CH(CH<sub>3</sub>) in-plane vibration.<sup>12,13</sup> Therefore, changes in the intensities of these two bands imply a more planar structure of BV in the complex. This is in line with the development of the band at 800 nm in UV-Vis spectrum (Fig. 1), which has been related previously to cyclic near-planar configuration of BV-metal complexes.<sup>15</sup>

originate from aggregation,<sup>17</sup> did not allow reliable assignment. However, this was of little relevance here, since the addition of copper ions led to a very strong effect - the complete loss of almost all lines. The loss of signals represents a result of strong paramagnetic effects that may come from an unpaired  $e^-$  that is delocalized in  $\pi$  orbitals of the ring/ligand, influencing all protons in the complex. The broadening of NMR signals beyond detection is not surprising considering that radicals are molecules with the longest electron relaxation time among paramagnetic species,<sup>18</sup> which leads to a large

nuclear relaxation rate. It is worth mentioning that  $^1\text{H}$  NMR lines of BV in deuterated DMSO were comparatively well resolved (ESI Fig. S6<sup>+</sup>), which points to an alteration of the protonation state and/or location, and in particular to different aggregation pattern. In addition, the lines were broadened but not lost (except for NH signals that could not be observed after  $\text{D}_2\text{O}$  addition because of chemical exchange) in the presence of even higher  $\text{Cu}^{2+}$  concentration (ESI Fig. S6<sup>+</sup>), underpinning the significant difference in BV/ $\text{Cu}^{2+}$  interactions in the two media. Low-T EPR was applied to further examine paramagnetic properties of the BV-Cu complex. The EPR spectrum of  $\text{Cu}^{2+}$  ( $S = 1/2$ ;  $I = 3/2$ ) in phosphate buffer shows that  $\text{Cu}^{2+}$  is weakly coordinated in an

**Figure 3.** Paramagnetic properties of BV-Cu systems in phosphate buffer (50 mM; pH 7.4). (a)  $^1\text{H}$  NMR spectra of BV (0.3 mM) with or without  $\text{Cu}^{2+}$  (0.15 mM) in the buffer prepared with  $\text{D}_2\text{O}$ . BV stock (20 mM) was prepared in DMSO. The acquisition of spectra was initiated after 5 min of incubation. (b) 30 K EPR spectra (perpendicular-mode) of 40  $\mu\text{M}$   $\text{Cu}^{2+}$  in the absence or the presence of BV (40 or 20  $\mu\text{M}$ ). Dashed line – the signal of the [BV]/[Cu] = 1 system divided by 2. (c) Room-T EPR spectrum of [BV]/[Cu] = 1 system. The spectrum was obtained via 10 accumulations (baseline corrected). Gray line - spectral simulation. (d) 25.5 K EPR spectra (parallel-mode) of 40  $\mu\text{M}$   $\text{Cu}^{2+}$  in the presence of 40  $\mu\text{M}$  BV ([BV]/[Cu] = 1). Power was 32 and 16 dB. For low-T EPR, samples were frozen in liquid  $\text{N}_2$  after 5 min incubation. (e) Excitation and emission fluorescence spectra of BV and [BV]/[Cu<sup>2+</sup>] = 1 system. The concentrations of BV and  $\text{Cu}^{2+}$  in the sample were 10  $\mu\text{M}$ . The acquisition of spectra was initiated after 5 min of incubation. (f) Fluorescence decay profile of BV and BV-Cu complex. Lifetime ( $\tau$ ) is presented as mean  $\pm$  standard deviation. (g) Emission spectra of BV ( $\lambda_{\text{ex}} = 381$  nm) and BV/ $\text{Cu}^{2+}$  ( $\lambda_{\text{ex}} = 386$  nm) at two temperatures. (h) Emission spectra of BV ( $\lambda_{\text{ex}} = 381$  nm) and BV/ $\text{Cu}^{2+}$  ( $\lambda_{\text{ex}} = 386$  nm) in the absence and the presence of 5 M urea.

The signals have been attributed to a highly delocalized electron.<sup>19,20</sup> In addition, the [BV]/[Cu<sup>2+</sup>] = 1 system showed a 9-line EPR spectrum at room T (Fig. 3c), as previously reported for porphyrin radical cation by Peeks and co-workers.<sup>19</sup> The simulation of this signal was performed assuming four equivalent  $^{14}\text{N}$  nuclei with an isotropic hyperfine coupling constant of 0.14 mT.<sup>19</sup> This speaks in favour of delocalization of unpaired electron over the complex center. Finally, parallel-mode EPR showed no signal (Fig. 3d). Furthermore, the spectra were run over a wide field range and no half field lines were observed, either in parallel or in perpendicular mode. These results are consistent with  $S = 0$  for the copper center.

Next, we compared the fluorescence of BV and BV-Cu complex (Fig. 3e-h). The [BV]/[Cu<sup>2+</sup>] = 1 system showed about two-fold stronger fluorescence than BV at equimolar concentration (Fig. 3e). Relative quantum yields for BV and BV-Cu complex were 0.86 and 0.95, respectively. However, the excitation and emission maxima, as well as the lifetimes (Fig. 3f), were next-to-identical, which implies that the fluorescence comes from the same fluorophore(s). To check whether the difference in fluorescence intensity is related to aggregation-caused quenching, we applied temperature increase and 5 M urea to induce deaggregation.<sup>17,21</sup> The increased fluorescence of BV under deaggregating conditions confirmed that BV forms aggregates in phosphate buffer (Fig. 3g, h), explaining the low resolution of  $^1\text{H}$  NMR spectrum of BV in the buffer (Fig. 3a). On the other hand, no changes were observed for BV-Cu complex, which implies that it did not form aggregates. This may be explained by a more planar structure and electrostatic repulsion by redistributed charge of the complex. It is important to note that the results obtained by fluorimetry further confirm that copper in the BV-Cu complex is not present in a paramagnetic form ( $\text{Cu}^{2+}$  with  $S = 1/2$ , or  $\text{Cu}^{3+}$  with  $S = 1$ ). The paramagnetic nature of  $\text{Cu}^{2+}$  (or  $\text{Cu}^{3+}$  with  $S = 1$  in analogy with  $\text{Ni}^{2+}$ ) would lead to quenching by enhancing the

axial symmetry with one  $g_{\perp}$  line and four lines coming from hyperfine coupling along  $g_{\parallel}$  (Fig. 3b). The addition of BV in equimolar concentration led to the loss of  $\text{Cu}^{2+}$  signal. In the [BV]/[Cu<sup>2+</sup>] = 0.5 system the double integral of the signal of  $\text{Cu}^{2+}$  in phosphate buffer was decreased by half, implying that an excess of copper is not bound to BV. The remaining signal in the [BV]/[Cu<sup>2+</sup>] = 1 system was broad, and did not show hyperfine structure. The  $g$ -value of the isotropic signal of BV-Cu complex was significantly lower than the average  $g$ -value of  $\text{Cu}^{2+}$  in the phosphate buffer indicating delocalization of the spin away from the metal nucleus. Similar EPR signals have been reported previously for porphyrin radical cation,<sup>19</sup> and for an oxidized copper-porphyrin model molecule complex.<sup>20</sup>

Further, redox properties of the complex were examined. BV showed a well-defined anodic peak at  $E_{\text{pa}1} = 117$  mV (Fig. 4a). Cyclic voltammogram of  $\text{Cu}^{2+}$  in phosphate buffer showed reversible redox behaviour at a peak potential at approximately -400 mV, with very weak currents. Therefore, the redox activity of BV-Cu systems in cyclic voltammograms was complex-centered. The [BV]/[Cu<sup>2+</sup>] = 2 system showed two additional oxidation peaks at much lower potentials than BV:  $E_{\text{pa}2} = -91$  mV and  $E_{\text{pa}3} = -341$  mV. The former potential corresponds to the oxidation of  $\text{Cu}^{1+}$ .<sup>23</sup> No reduction peaks could be observed. Differential pulse voltammetry delivered similar results – the [BV]/[Cu<sup>2+</sup>] = 2 system showed two additional peaks, most likely coming from two  $1e^-$  oxidations (Fig. 4b). It is noteworthy that a similar oxidation pattern has been observed previously for a complex of BV model compound with copper.<sup>24</sup> A direct linear relationship between  $I$  and the square root of scan rate imply that the currents mainly depend on two parameters: the rate at which redox species diffuse to the electrode surface ( $D$ ), and the rate constant of electron transfer (ESI Fig. S7<sup>+</sup>). Other interactions, for example adsorption, were negligible.<sup>25</sup> BV showed significantly higher  $D$  compared to  $D$  values that were calculated for the two other peak currents. A faster diffusion of BV to the electrode surface in comparison to the BV-Cu complex was expected, since BV has more negative charge (two deprotonated carboxyl groups), than the complex formed with positive copper ion (total charge is zero). Oximetry was applied to examine the possibility that an electron is lost in the reaction between BV and  $\text{Cu}^{2+}$ , as proposed previously for complexes of copper ions with BV model molecules in organic solvents.<sup>5,26</sup> In the aqueous system that was applied here, molecular oxygen represents the main  $e^-$  acceptor. It may be directly involved in redox reaction between BV and  $\text{Cu}^{2+}$ , or it may be reduced by  $\text{Cu}^{1+}$ , which is unstable under physiological

settings. There was a slight consumption of  $O_2$  in  $[BV]/[Cu^{2+}] = 1$  system during the process (Fig. 4c), which may be explained by traces of 'free' copper as discussed (see Fig. 1 and ESI Fig. S2<sup>†</sup>). However, in the presence of an excess of copper ( $[BV]/[Cu^{2+}] = 0.5$ ), the consumption of  $O_2$  was significant. This implies that 'free'  $Cu^{2+}$  reacts with the complex and 'shuttles' an  $e^-$  to  $O_2$ . The addition of catalase to  $[BV]/[Cu^{2+}]$  systems after 15 min incubation, resulted in  $O_2$  release, implying that hydrogen peroxide is accumulated. The concentration of accumulated  $H_2O_2$  corresponded to the amount of  $O_2$  that was consumed in the  $[BV]/[Cu^{2+}] = 1$  system and to approximately half of  $O_2$  consumed in the  $[BV]/[Cu^{2+}] = 0.5$  system. As an illustration of the redox mechanism, we added  $Cu^{1+}$  to the buffer.  $Cu^{1+}$  rapidly reduced  $O_2$  to produce superoxide radical anion resulting in  $O_2$  concentration drop, which was partially reversed by catalase. Further analysis of stoichiometry could not be performed because the system composed of transition metal, reactive oxygen species and organic molecule involves multiple reactions that resulted in fragmentation of BV (see ESI Fig. S5<sup>†</sup>).

**Figure 4.** Redox properties of BV/Cu systems in phosphate buffer (50 mM; pH 7.4). (a) Cyclic voltammograms of BV and BV-Cu complex at a boron-doped diamond electrode (scan rate 0.1 V/s). Concentrations of BV and  $Cu^{2+}$  were 0.4 mM and 0.2 mM, respectively. Oxidation/anodic peak current potentials ( $E_{pa}$ ) are labeled. (b) Differential pulse voltammograms (increment, 0.004 V; pulse width, 0.05 s; sample width, 0.01 s; quiet time, 2 s). (c) Consumption of molecular oxygen in BV solutions following addition of  $Cu^{2+}$ , or the addition of  $Cu^{1+}$  to phosphate buffer. The trace without Cu addition is presented for reference. In all experiments  $[BV] = 200 \mu M$ . Catalase (200 IU) was added 15 min after copper addition, to quantify the accumulation of  $H_2O_2$  ( $2 H_2O_2 \rightarrow O_2 + 2H_2O$ ). Concentrations of  $H_2O_2$  were as follows: 4  $\mu M$  (red trace), 18  $\mu M$  (blue), 45  $\mu M$  (green), and 75  $\mu M$  (magenta). (d) UV-Vis spectra of BV with  $Cu^{2+}$  and  $Cu^{1+}$  under anaerobic and aerobic conditions. The signals are compared to the spectra of analogous BV/ $Cu^{2+}$  systems.  $Cu^{1+}$  does not show detectable absorbance at the applied concentration. (e) The effects of reducing agent – ascorbate (Asc) on BV-Cu complex. (f) The effects of oxidizing agent –  $KMnO_4$  on BV-Cu complex. Both, Asc and  $KMnO_4$  did not affect the spectrum of free BV.

Next, the effects of reducing ( $Cu^{1+}$  and ascorbate) and oxidizing ( $KMnO_4$ ) agents on BV-Cu complex were examined. The complex was not affected by  $Cu^{1+}$  (Fig. 4d). BV was exposed to 1/1 mixture of  $Cu^{1+}$  and  $Cu^{2+}$  under anaerobic conditions. The spectrum of 20  $\mu M$  BV with 10  $\mu M$   $Cu^{2+}$  and 10  $\mu M$   $Cu^{1+}$  corresponded to the spectrum of an analogous  $[BV]/[Cu^{2+}] = 2$  system. Initially present  $Cu^{1+}$  did not affect the spectrum, *i.e.* the system was stable. When exposed to air,  $Cu^{1+}$  was oxidized by  $O_2$  to produce  $Cu^{2+}$  that reacted with free BV, resulting in the production of an additional amount of complex. The complex was not affected by ascorbate as well (Fig. 4e). On the other hand, the complex was degraded by  $KMnO_4$ , whereas this strong oxidizing species did not affect free BV (Fig. 4f). The results presented here imply that BV and  $Cu^{2+}$  react under physiological settings to produce 1:1 complex which is composed of  $Cu^{1+}$  and BV radical cation ( $BV^{•+}$ ) or  $Cu^{3+}$  and BV radical anion ( $BV^{•-}$ ). It should be stressed that the proposed distribution of electrons is formal, and that the unpaired  $e^-$  may be delocalized over the entire molecule. The delocalized unpaired electron remains on the ring, whereas copper is bound to N in pyrroles. The presence of an unpaired delocalized  $e^-$  and the development of  $BV^{•+}$  or  $BV^{•-}$  are implicated by: (i) the results of Raman spectroscopy that

implied a higher stability of BV in the complex that is provided by an additional delocalization of  $\pi$ -electronic cloud; (ii) NMR data showing strong paramagnetism of the complex; and (iii) perpendicular-mode EPR spectra. The proposed redox state of copper in the complex –  $Cu^{1+}$  or  $Cu^{3+}$  is suggested by parallel-mode EPR and fluorescence results that were consistent with  $S = 0$ . At this point,  $BV^{•+}$ - $Cu^{1+}$  appears to be a more probable structure of the complex. This is implicated by: (i) the oxidation peak in cyclic voltammogram of BV-Cu complex that corresponds to  $Cu^{1+}$  oxidation (ii) the EPR signals that were previously attributed to porphyrin radical cation;<sup>19</sup> and (iii) the susceptibility of the complex to oxidizing and not to reducing agents, since it appears more plausible that metal center and not delocalized  $e^-$  represents the main site of redox interactions of the complex. However, both possibilities remain open. Finally, it is important to point out that BV-Cu complex in aqueous buffer differs distinctly than in organic solvents, such as DMSO or chloroform. Balch and co-workers have shown that BV analog and  $Cu^{2+}$  in chloroform build a ferromagnetically coupled  $S = 1$   $Cu^{2+}$ /BV radical cation system or a  $S = 1$   $Cu^{3+}$  BV trianion system.<sup>5a</sup> The complex showed  $^1H$  NMR spectrum that spread over -150–100 ppm region and no EPR spectrum (perpendicular mode) at room T, and it was susceptible to reduction by ascorbate.<sup>5a</sup> The explanation for the development of different complexes may lay in different properties of solvents, which may affect the stability of specific conformation or may even act as ligands,<sup>27</sup> but also in different electron distribution within BV and BV analog molecules.

## Conclusions

At physiological pH, BV builds a complex with copper ions in 1:1 stoichiometry. The formation of the complex involves the rearrangement of electronic structure which provides increased energetic stability and strong paramagnetic effects. We believe that a complex with highly delocalized unpaired  $e^-$  and the formal  $BV^{•+}$ - $Cu^{1+}$  or  $BV^{•-}$ - $Cu^{3+}$  character best suites the outlined properties. The presented results may shed new light on long-standing issues of BV chemistry and catalysis in biological systems.

## Experimental

### Chemicals

All chemicals were of analytical grade: BV, buffer components, dimethyl sulfoxide (DMSO), DMSO- $d_6$  (deuterated DMSO, 99.9 % D atom),  $D_2O$  (99.9% D atom), and urea were purchased from Sigma-Aldrich (St. Louis, MO, USA);  $CuCl_2$  was from Merck (Kenilworth, NJ, USA); solvents for MS (acetonitrile, formic acid; LC-MS grade) were obtained from Fisher Scientific (Loughborough, UK). All experiments were performed using bidistilled deionized water (18 M $\Omega$ ) that was obtained by reagent grade water system (Millipore, Billerica, USA). Stock solutions of BV - 20 mM in DMSO for experiments with high final concentrations (NMR, Raman, cyclic voltammetry) or 1 mM in 5 mM NaOH for all other experiments were prepared

daily and kept on ice in the dark. Phosphate buffer - 50mM  $\text{KH}_2\text{PO}_4$  with pH adjusted to 7.4 with KOH, was prepared daily.

#### UV-VIS spectroscopy

UV-Vis absorption spectra were obtained using a 2501 PC Shimadzu spectrophotometer (Kyoto, Japan). Sample volume was 1 mL. Scan time was 50 s. Samples were freshly prepared and immediately scanned at wavelengths from 800 to 200 nm at room T. Changes of spectra were monitored for 60 min. Each system was prepared in light-protected glass and stirred. Aliquots were measured and discarded for each time-point, since we noted that irradiation during the collection of UV-Vis spectra may result in BV degradation.

#### HESI-MS spectrometry

MS analysis was performed using a TSQ Quantum Access Max mass spectrometer equipped with a HESI source, which was used with ion source settings as follows: spray voltage, 3500 V; sheath gas,  $\text{N}_2$ ; pressure, 30 AU; ion sweep gas pressure, 3 AU; auxiliary gas ( $\text{N}_2$ ) pressure, 10 AU; vaporizer temperature, 450°C; capillary temperature, 380°C; skimmer offset, 0 V. Multiple mass spectrometric data were acquired in positive mode, including full scanning in  $m/z$  range from 100 to 1000 (FS) for qualitative analysis and product ion scanning (PIS) mode for the quantitative analysis. Collision-induced fragmentation experiments were performed using Ar as the collision gas, with collision energy set at 5 eV. SRM experiments for quantitative analysis was performed using two MS2 fragments for each compound, which were previously defined as dominant in PIS experiments. Samples were introduced into the mass spectrometer with a syringe pump and continuous flow injection for a period of 5 min at a flow rate of 5.0  $\mu\text{L}/\text{min}$ . Analyst version 1.4 of Xcalibur software (Thermo Fisher Scientific, Waltham, MA, USA) was used for data acquisition and processing.

#### Raman spectroscopy

The Raman spectra of sample solutions were recorded on a Thermo DXR Raman microscope (Thermo Fisher Scientific). Sample aliquots of 5  $\mu\text{L}$  were placed on the Raman grade calcium fluoride holder following the adjustment and stabilization of pH of the solution and Raman spectra were recorded. The 532 nm laser excitation line was used, with the following settings: exposure time, 10 s; number of exposures, 10; grating, 900 lines/mm; pinhole, 50  $\mu\text{m}$ ; laser power at the sample, 2 MW.

#### Fluorescence Spectroscopy

Fluorescence spectra were acquired using a Fluorolog FL3-221 with a 450 mW Xe lamp (Jobin Yvon Horiba, Paris, France), and FluorEssence 3.5 software (Horiba Scientific, Kyoto, Japan), and the following settings: excitation range, 320–380 nm; emission range, 400–600 nm; increment, 2 nm; slit (band pass), 3 nm for establishing excitation and emission spectra, and 1 nm for acquiring emission spectra at 293 K and 328 K, and emission spectra in the presence of urea (5 M). Emission detector signal was scaled by reference quantum counter

signal (S1c/R1c). Relative quantum yield was determined from emission and excitation spectra using FluorEssence 3.5 software. Lifetime was calculated from fluorescence decay profile which was established using excitation nano-led diode (380 nm). The emission was detected at 470 nm and 480 nm for BV and BV/Cu system, respectively. The decay was fitted using 3 exponentials.

#### $^1\text{H}$ NMR Spectroscopy

$^1\text{H}$  NMR spectra of BV (0.3 mM) in the absence or in the presence of  $\text{CuCl}_2$  (0.3 mM) were recorded on a Bruker Avance III 500 spectrometer with TopSpin v3.2 interface, using 5 mm BBO probe-head, at 298 K. All samples (and solutions) were prepared in  $\text{D}_2\text{O}/\text{DMSO-d}_6$  and placed in 5-mm quartz tubes. Residual HDO signal at 4.7 ppm was used as chemical shift reference. Spectra were analyzed in MestReNova 12.0.1 (Mestrelab Research, Santiago de Compostela, Spain).

#### EPR Spectroscopy

Perpendicular-mode EPR spectra at 30 K were recorded on a Bruker Elexsys-II EPR spectrometer operating at X-band (9.616 GHz), using the following conditions: power, 32 dB; modulation amplitude, 0.8 mT; modulation frequency, 100 kHz. Parallel-mode signals were obtained at 25.5 K, using a Bruker EMXplus spectrometer operating at X-band (9.272 GHz) with the dual-mode cavity, and the following settings: power, 16 or 32 dB; modulation amplitude, 1 mT; modulation frequency, 20 kHz. Samples were placed in quartz EPR tubes and quickly frozen in cold isopentane following 5 min incubation period under anaerobic conditions. All spectra were non-saturated, baseline corrected, and showed no signs of freezing-induced sample inhomogeneity.<sup>28</sup> Measurements at room T were conducted on a Varian E104 operating at X-band (9.51 GHz), using the following settings: microwave power, 20 mW; modulation amplitude, 0.2 mT; modulation frequency, 100 kHz. Spectra were obtained under aerobic conditions. The simulation of the room T EPR spectrum was performed in WINEPR SimFonia software (Bruker Analytische Messtechnik GmbH, Darmstadt, Germany), using previously described parameters.<sup>19</sup>

#### Oximetry

Concentration of  $\text{O}_2$  in samples was measured/monitored using a Clark type oxygen electrode (Hansatech Instruments Ltd., King's Lynn, UK) operating with Lab Pro interface and Logger Pro 3 software (Vernier, Beaverton, OR, USA). All systems were recorded for 2-5 min before the addition of Cu to establish the stability of baseline and zero rate of  $\text{O}_2$  change at room T.

#### Cyclic voltammetry and differential pulse voltammetry

The voltammetric measurements were performed using a potentiostat/galvanostat CHI 760b (CH Instruments, Inc, Austin, TX, USA). The electrochemical cell (total volume of 3 mL) was equipped with a boron-doped diamond electrode (surface area 7.07  $\text{mm}^2$ ; Windsor Scientific LTD, UK; declared performances: resistivity, 0.075  $\Omega$  cm; boron doping level,

1000 ppm), as the working electrode, an Ag/AgCl (3M KCl) and platinum wire as reference and counter electrode, respectively. All potentials reported in this paper are referred versus this electrode. Scan rate was 0.1 V/s. Differential pulse voltammetry was performed on the same instrument using the following settings: initial  $E$ , -1 V; final  $E$ , 1 V; increment, 0.004 V; amplitude, 0.05 V; pulse width, 0.05 s; sample width, 0.01 s; quiet time, 2 s. Measurements were initiated immediately after sample preparation and performed at room T.

### Conflicts of interest

There are no conflicts to declare.

### Acknowledgements

This work was supported by the Ministry of Education, Science and Technological Development of the Republic of Serbia (III43010). We acknowledge networking support from the COST Action FeSBioNet (Contract CA15133). We are thankful to Ana Popović-Bijelić and Miloš Mojović at EPR Laboratory, Faculty of Physical Chemistry, University of Belgrade. D.M.S was supported by Magbiovin project (FP7-ERA Chairs-Pilot Call-2013, Grant Agreement: 621375).

### Notes and references

- (1) L. Zhang, *Heme Biology: The Secret Life of Heme in Regulating Diverse Biological Processes*, World Scientific Publishing Company, Singapore, 2011.
- (2) D. Chen, J. D. Brown, Y. Kawasaki, J. Bommer, J. Y. Takemoto, *BMC Biotechnol.*, 2012, **12**, 89.
- (3) (a) C. Cornelius, *Biliverdin in Biological Systems*. In *One Medicine*; ed. O. Ryder, M. Byrd, Springer, Berlin, 1984, 321–334. (b) J. Nam, Y. Lee, Y. Yang, S. Jeong, W. Kim, J. W. Yoo, S. Jon, J. O. Moona, C. Lee, H. Y. Chunga, M. S. Kima, S. Jonb, Y. Jung, *Free Radic. Biol. Med.*, 2018, **124**, 232–240.
- (4) (a) K. Nguyen, S. Rath, L. Latos-Grazyński, M. Olmstead, A. Balch, *J. Am. Chem. Soc.*, 2004, **126**, 6210–6211; (b) C. Li, B. Kräutler, *Dalton Trans.*, 2015, **44**, 10116–10127. (c) A. L. Balch, M. Mazzanti, B. C. Noll, M. M. Olmstead, *J. Am. Chem. Soc.*, 1994, **116**, 9114–9122; (d) A. L. Balch, B. C. Noll, E. P. Zovinka, *J. Am. Chem. Soc.*, 1992, **114**, 3380–3385; (f) I. Spasojević, I. Batinić-Haberle, R. D. Stevens, P. Hambright, A. N. Thorpe, J. Grodkowski, P. Neta, I. Fridovich, *Inorg. Chem.*, 2001, **40**, 726–739.
- (5) (a) A. L. Balch, M. Mazzanti, B. C. Noll, M. M. Olmstead, *J. Am. Chem. Soc.*, 1993, **115**, 12206–12207; (b) I. Sóvágó, B. Harman, I. Kolozsvári, F. Matyuska, *Inorg. Chim. Acta.*, 1985, **106**, 181–186.
- (6) I. Goncharova, M. Urbanová, *Anal. Biochem.*, 2009, **392**, 28–36.
- (7) (a) S. F. Asad, S. Singh, A. Ahmad, S. M. Hadi, *Biochim. Biophys. Acta*, 1999, **1428**, 201–208; (b) F. S. Asad, S. Singh, A. Ahmad, N. U. Khan, S. M. Hadi, *Chem. Biol. Interact.*, 2001, **137**, 59–74.
- (8) (a) B. E. Fischer, U. K. Haring, R. Tribolet, H. Sigel, *Eur. J. Biochem.*, 1979, **94**, 523–530; (b) J. Nagaj, K. Stokowa-Sołtys, E. Kurowska, T. Frączyk, M. Jeżowska-Bojczuk, W. Bal, *Inorg. Chem.*, 2013, **52**, 13927–13933.
- (9) D. A. Lightner, D. L. Holmes, A. F. McDonagh, *J. Biol. Chem.*, 1996, **271**, 2397–2405.
- (10) (a) A. F. McDonagh, L. A. Palma, *Biochem. J.*, 1980, **189**, 193–208; (b) D. Krois, H. Lehner, *J. Chem. Soc. Perkin Trans. 2*, 1993, **7**, 1351–1360.
- (11) S. Phillips, B. C. Noll, M. M. Olmstead, A. L. Balch, *Can. J. Chem.*, 2001, **79**, 922–929.
- (12) (a) F. Celis, M. M. Campos-Vallette, J. S. Gómez-Jeria, R. E. Clavijo, G. P. Jara, C. Garrido, *Spectrosc. Lett.*, 2016, **49**, 336–342; (b) J. He, X. D. Lu, X. Zhou, N. T. Yu, Z. Chen, *Biospectroscopy*, 1995, **1**, 157–162; (c) J. Hu, T. Wang, D. Moigno, M. Wumaier, W. Kiefer, J. Mao, Q. Wu, F. Niu, Y. Gu, Q. Chen, J. Ma, H. Feng, *Spectrochim. Acta A Mol. Biomol. Spectrosc.*, 2001, **57**, 2737–2743; (d) J. M. Hu, E. J. Liang, F. Duschek, W. Kiefer, *Spectrochim. Acta A: Mol. Biomol. Spectrosc.*, 1997, **53**, 1431–1438.
- (14) (a) J. Chen, J. M. Hu, R. S. Sheng, *Spectrochim. Acta, Part A*, 1994, **50**, 929–936. (b) S. Tao, L. J. Yu, D. Y. Wu, Z. Q. Tian, *Acta Phys. Chim. Sin.*, 2013, **29**, 1609–1617.
- (15) J. H. Fuhrhop, A. Salek, J. Subramanian, C. Mengersen, S. Besecke, J. Liebig, *Ann. Chem.*, 1975, **6**, 1131–1147.
- (16) L. Sztterenber, L. Latos-Grazyński, J. Wojaczyński, *Chem. Phys. Chem.*, 2003, **4**, 691–698.
- (17) M. Feliz, J. M. Ribó, A. Salgado, F. R. Trull, M. A. Valló, *Monatshefte. Chemie.*, 1989, **120**, 445–451.
- (18) (a) I. Bertini, C. Luchinat, G. Martini, *Handbook of Electron Spin Resonance*, American Institute of Physics, New York, 1994; (b) I. Bertini, C. Luchinat, G. Parigi, *Solution NMR of Paramagnetic Molecules: Applications to Metallobiomolecules and Models*, Elsevier, Amsterdam, 2001.
- (19) M. D. Peeks, C. E. Tait, P. Neuhaus, G. M. Fischer, M. Hoffmann, R. Haver, A. Cnossen, J. R. Harmer, C. R. Timmel, H. L. Anderson, *J. Am. Chem. Soc.*, 2017, **139**, 10461–10471.
- (20) G. M. Godziela, H. M. Goff, *J. Am. Chem. Soc.*, 1986, **108**, 2237–2243.
- (21) M. Rahman, H. J. Harmon, *J. Porphy. Phthalocyanines*, 2007, **11**, 125–129.
- (22) (a) G. Sivaraman, M. Iniya, T. Anand, N. G. Kotla, O. Sunnapu, S. Singaravadevel, A. Gulyani, D. Chellappa, *Coord. Chem. Rev.*, 2018, **357**, 50–104; (b) Y. Chen, J. Jiang, *Org. Biomol. Chem.*, 2012, **10**, 4782–4787; (c) K. Kano, T. Sato, S. Yamada, T. Ogawa, *Phys. Chem.*, 1983, **87**, 566–569; (d) J. Prabphal, T. Vilaivan, T. Praneenarat, *Chemistry. Select.*, 2018, **3**, 894–899.
- (23) B. Božić, J. Korać, D. M. Stanković, M. Stanić, A. Popović-Bijelić, J. Bogdanović Pristov, I. Spasojević, M. Bajčetić, *Chem. Biol. Interact.*, 2017, **278**, 129–134.
- (24) A. J. Pistner, R. C. Pupillo, G. P. P. Yap, D. A. Lutterman, Y. Z. Ma, J. Rosenthal, *J. Phys. Chem. A*, 2014, **118**, 10639–10648.
- (25) J. Sochr, Ľ. Švorc, M. Rievaj, D. Bustin, *Diam. Relat. Mater.*, 2014, **43**, 5–11.
- (26) R. Koerner, M. M. Olmstead, A. Ozarowski, S. L. Phillips, P. M. Van Calcar, K. Winkler, A. L. Balch, *J. Am. Chem. Soc.*, 1998, **120**, 1274–1284.
- (27) E. Sinn, *Inorg. Nucl. Chem. Lett.* 1970, **6**, 811–815.
- (28) W. R. Hagen, *Biomolecular EPR Spectroscopy*, CRC Press, Boca Raton, 2008.

## Journal Name

## ARTICLE

Table of content: In physiological settings, biliverdin and Cu<sup>2+</sup> build a paramagnetic complex with formal structure: radical cation/Cu<sup>1+</sup> or radical anion/Cu<sup>3+</sup>.

View Article Online  
DOI: 10.1039/C8DT04724C

Dalton Transactions Accepted Manuscript